





Epac1 null mice have nephrogenic diabetes insipidus with deficient corticopapillary osmotic gradient and weaker collecting duct tight junctions

Kathrine Sivertsen Åsrud¹  | Ronja Bjørnstad¹ | Reidun Kopperud¹ | Line Pedersen¹ | Barbara van der Hoeven¹ | Tine V. Karlsen¹ | Cecilie Brekke Rygh^{1,2} | Fitz-Roy Curry³ | Marit Bakke¹ | Rolf K. Reed^{1,4}  | Olav Tenstad¹  | Stein O. Døskeland¹ 

¹Department of Biomedicine, Faculty of Medicine, University of Bergen, Bergen, Norway

²Faculty of Health and Social Sciences, Western Norway University of Applied Sciences, Bergen, Norway

³Department of Physiology and Membrane Biology, School of Medicine, University of California, Davis, CA, USA

⁴Centre for Cancer Biomarkers, University of Bergen, Bergen, Norway

Correspondence

Stein O. Døskeland, Department of Biomedicine, University of Bergen, Jonas Lies vei 91, N-5009 Bergen, Norway.
Email: Stein.Doskeland@uib.no

Present address

Ronja Bjørnstad and Reidun Kopperud, Department of Clinical Science, University of Bergen, Bergen, Norway

Funding information

This work was supported by grants from Kreftforeningen (811164), the Norwegian Research Council (NRC) (22325) and the Regional Health Authorities (Helse-Vest) (911979, 99080, 911974, 911666) to SD, OT and RR, and from NIH (HL028607-32) to FC.

Abstract

Aim: The cAMP-mediator Epac1 (*RapGef3*) has high renal expression. Preliminary observations revealed increased diuresis in Epac1^{-/-} mice. We hypothesized that Epac1 could restrict diuresis by promoting transcellular collecting duct (CD) water and urea transport or by stabilizing CD paracellular junctions to reduce osmolyte loss from the renal papillary interstitium.

Methods: In Epac1^{-/-} and Wt C57BL/6J mice, renal papillae, dissected from snap-frozen kidneys, were assayed for the content of key osmolytes. Cell junctions were analysed by transmission electron microscopy. Urea transport integrity was evaluated by urea loading with 40% protein diet, endogenous vasopressin production was manipulated by intragastric water loading and moderate dehydration and vasopressin type 2 receptors were stimulated selectively by i.p.-injected desmopressin (dDAVP). Glomerular filtration rate (GFR) was estimated as [¹⁴C]inulin clearance. The glomerular filtration barrier was evaluated by urinary albumin excretion and microvascular leakage by the renal content of time-spaced intravenously injected ¹²⁵I- and ¹³¹I-labelled albumin.

Results: Epac1^{-/-} mice had increased diuresis and increased free water clearance under antidiuretic conditions. They had shorter and less dense CD tight junction (TJs) and attenuated corticomedullary osmotic gradient. Epac1^{-/-} mice had no increased protein diet-induced urea-dependent osmotic diuresis, and expressed Wt levels of aquaporin-2 (AQP-2) and urea transporter A1/3 (UT-A1/3). Epac1^{-/-} mice had no urinary albumin leakage and unaltered renal microvascular albumin extravasation. Their GFR was moderately increased, unless when treated with furosemide.

Conclusion: Our results conform to the hypothesis that Epac1-dependent mechanisms protect against *diabetes insipidus* by maintaining renal papillary osmolarity and the integrity of CD TJs.

Kathrine Sivertsen Åsrud and Ronja Bjørnstad have contributed equally to this work.

This is an open access article under the terms of the Creative Commons Attribution License, which permits use, distribution and reproduction in any medium, provided the original work is properly cited.

© 2020 The Authors. *Acta Physiologica* published by John Wiley & Sons Ltd on behalf of Scandinavian Physiological Society

KEYWORDS

collecting duct, diabetes insipidus, exchange protein directly activated by cAMP (Epac1, *RapGef3*), GFR, occluding junction, vasopressin (AVP)

1 | INTRODUCTION

The second messenger cAMP has two generally expressed mediators: The cAMP-dependent protein kinase (*PRKAC/R*; PKA) and the cAMP-activated Rap GDP exchange factors Epac1 and Epac2 (*RapGef3*, 4).^{1–5} Epac1 (*RapGef3*) has high renal expression.^{6–8} We noted earlier that our Epac1^{−/−} mice had ‘wet’ cages caused by increased diuresis.⁹ The available evidence summarized below suggested two working hypotheses for how Epac1 could limit diuresis: (a) by enhancing urea and water transport in the collecting duct (CD); and (b) by regulating CD tight junction (TJ) integrity to minimize osmolyte loss from the renal papillary interstitium.

In vitro studies using the Epac-stimulating cAMP analogue 8-pPCT-2'-O-Me-cAMP^{10,11} suggest that Epac can stimulate transcellular urea transport,^{5,12,13} maintain high aquaporin-2 (AQP-2) synthesis^{5,14} and stimulate the insertion of AQP-2 in the principal cell (PC) apical membrane.¹⁵

8-pPCT-2'-O-Me-cAMP has numerous ‘off-target’ actions. It can affect purinergic receptors or transmembrane transporters and indirectly activate PKA by inhibiting cAMP degradation.^{16,17} To evaluate specific Epac1 actions, the present study compares Wt and Epac1 null mice. The Epac1^{−/−} mice have been described previously and do not express Epac1 in any tested tissue, including kidney.⁷

Early data based on immunofluorescence suggested high Epac1 expression in the proximal tubules and the intercalated cells (IC) of the CD.⁹ More recent, quantitative transcriptomic studies indicate low expression in proximal tubules and high expression in renal glomeruli and the CD,⁶ whose PC express more *RapGef3* than the ICs.¹⁰

The reports that Epac1 contributes to the cAMP induction of urea transporters^{5,11,12} imply that Epac1 can protect against urea-induced osmotic diuresis. If so, a high protein load^{14,18} should induce more severe diuresis in the Epac1^{−/−} mice. We compared, therefore, the diuresis of Wt and Epac1^{−/−} mice on low (4%), standard (12.5%) or high (40%) protein diet, and determined if Epac1-deficient mice had altered expression of the major urea transporter (UT-A1). We determined also whether their AQP-2 expression was decreased based on reports that Epac1 may contribute to enhanced AQP-2 synthesis or stability.^{5,14}

The high Epac1 expression in renal glomeruli⁶ suggests that Epac1 can affect glomerular function. We tested, therefore, if the Epac1 null mice had deficient glomerular filtration barrier, or had altered glomerular filtration rate (GFR)

in the absence or presence of the tubuloglomerular feedback (TGF)^{19,20} blocker furosemide.^{19,21}

Several Epac1^{−/−} mouse organs have increased basal in vivo microvascular permeability,^{7,22} indicating that Epac1 can limit fluid extravasation. We hypothesized that Epac1 might act to conserve intravascular fluid also via renal actions. We therefore compared the diuresis of Wt and Epac1^{−/−} mice not only under basal conditions, but also after water loading (WL) when endogenous AVP is low,²³ after moderate water deprivation and after injection of the avpr2 receptor agonist desmopressin (dDAVP).

A number of observations suggest that the CD cell junctional complexes (JCs) could be targets for regulation by Epac1. Firstly, Epac1 is well known to strengthen cell junctions in vitro^{24,25} and in vivo.⁷ Secondly, Epac1 and its major downstream target E-cadherin have higher expression in the CD than in other parts of the rat nephron, as shown by deep sequencing of mRNA from dissected rat nephron segments.⁶ The importance of E-cadherin for an intact CD barrier and ability to concentrate urine are demonstrated by mice with downregulated Grainyhead-like protein 2 homolog (GRHL2). They express less key junctional proteins and have *diabetes insipidus* as well as decreased renal medullary Na⁺ content.²⁶ We therefore determined the Na⁺ content in snap-frozen renal papillae from Wt and Epac1^{−/−} mice and studied the CD junctions by transmission electron microscopy (TEM).

2 | RESULTS

2.1 | Epac1^{−/−} mice have increased diuresis at normal and low urea load

The deletion of Epac1 did not impact kidney weight (average 262 mg in Wt and 263 mg in Epac1^{−/−} mice), kidney-to-BW ratio (10.3 mg g^{−1} in either Wt or Epac1^{−/−}) or gross renal morphology (Table S1, Figure S1). However, cages housing Epac1^{−/−} mice were consistently ‘wetter’ than cages housing Wt mice under standard breeding conditions. Specifically, Epac1 null mice housed in metabolic cages with free access to standard (12.5%) protein chow and drinking water had more than twice as high diuresis as matched Wt mice (Table 1).

To test whether the increased Epac1^{−/−} mouse diuresis was related to deficient handling of urea, we compared the effect of low (4%) and high (40%) protein. The diuretic phenotype was strongest at 4% protein diet (Table 2A). The 40% protein

TABLE 1 24-h baseline water consumption, diuresis and key urinary parameters for Wt and *Epac1*^{-/-} mice fed standard (12.5%) protein diet

Variable determined	(12.5%) protein content	
	Wt mice (n = 6)	<i>Epac1</i> ^{-/-} mice (n = 6)
Body weight (g)	20.4 (SD1.3)	21.4 (SD1.9)
Water consumption (μL 24h ⁻¹ g ⁻¹)	195 (SD110)	242 (SD81)
Urine output (μL 24h ⁻¹ g ⁻¹)	59.8 (SD15)	130 (SD33) ^{aaaa}
Urine osmolality (mOsm kg ⁻¹ H ₂ O)	1770 (SD698)	1360 (SD808)
Osm excr.(nosm min ⁻¹ g ⁻¹)	77.8 (SD23.6)	146 (SD93.7)
Urine urea conc. (mmol/L)	1330 (SD520)	1150 (SD713)
Urea excr. (nmol min ⁻¹ g ⁻¹)	64.1 (SD15.9)	60.7 (SD24.6)

The mice were kept in metabolic cages for 24 h with free access to drinking water and chow containing 12.5% protein. Urine was continuously sampled throughout the 24-h period. The table shows the mean (SD) water consumption (n = 13-14), urine output (n = 13-14) and selected urinary parameters (n = 6). Unpaired two-tailed Student's *t* test with Welch's correction or non-parametric Mann-Whitney test was used to determine statistical differences between the diuresis of Wt and *Epac1*^{-/-} mice, ^{aaaa}*P* < .0001, sum of ranks 105, 273, Mann-Whitney *U* = 0.

TABLE 2 Urinary Parameters for Wt and *Epac1*^{-/-} mice on low (4%) and high (40%) protein diet

Variable determined	(A) Low protein diet (4%)		(B) High protein diet (40%)	
	WT	<i>Epac1</i> ^{-/-}	WT	<i>Epac1</i> ^{-/-}
Body weight (g)	19.7 (SD2.1)	21.1 (SD2.1)	19.0 (SD3.1)	21.8 (SD1.8)
Water consumed (μL 24h ⁻¹ g ⁻¹)	110 (SD24)	179 (SD18) ^{aa}	227 (SD42)	239 (SD60)
Urine output (μL 24h ⁻¹ g ⁻¹)	50.6 (SD13)	110 (SD14) ^{bbb}	165 (SD68.4)	181 (SD54.7)
Urine Urea (mmol/L)	874 (SD219)	504 (SD146) ^c	2667 (SD434)	2619 (SD1389)
Urine Na ⁺ (mmol/L)	154 (SD37)	68 (SD5) ^d	42 (SD9)	37 (SD8)
Urine K ⁺ (mmol/L)	262 (SD71)	138 (SD14) ^e	108 (SD23)	92 (SD26)
Urine Creatinine (mmol/L)	3.56 (SD1.00)	1.82 (SD0.12) ^f	1.27 (SD0.48)	1.18 (SD0.32)
Urine osm. (mosm kg ⁻¹)	2091 (SD468)	1046 (SD128) ^{gg}	4249 (SD903)	3268 (SD554)
Urea excr. (nmol min ⁻¹ g ⁻¹)	31.9 (SD7.0)	38.0 (SD7.6)	290 (SD82)	298 (SD68)
Na ⁺ excr. (nmol min ⁻¹ g ⁻¹)	5.32 (SD1.04)	5.24 (SD0.56)	4.45 (SD0.92)	4.53 (SD0.93)
K ⁺ excr. (nmol min ⁻¹ g ⁻¹)	9.37 (SD1.5)	10.6 (SD0.88)	11.1 (SD2.62)	11.0 (SD1.78)
Creat. excr. (pmol min ⁻¹ g ⁻¹)	117 (SD13)	140 (SD15.7)	128 (SD8.4)	139 (SD17.4)
Plasma urea (mmol/L)	2.1 (SD0.23)	2.0 (SD0.13)	3.6 (SD0.42)	2.9 (SD0.39)
Plasma creatinine (μmol/L)	7.8 (SD0.5)	7.3 (SD2.0)	6.1 (SD0.9)	5.4 (SD2.0)
Urea clearance (μL min ⁻¹)	74 (SD15)	104 (SD19) ^h	402 (SD99)	569 (SD130)
Creatinine clearance (μL min ⁻¹)	360 (SD57)	447 (SD29)	418 (SD17)	512 (SD66)

Wt (n = 4-5) and *Epac1*^{-/-} mice (n = 4-5) were first (A) fed 7 d 4% protein diet followed by 24 h determination of water intake and diuresis, and next (B) 7 d 40% protein diet followed by similar monitoring. The results are given as mean (SD), and excretion data are normalized per g body weight. Unpaired two-tailed Student's *t* test with Welch's correction when applicable, was used to determine statistical differences between the diuresis of Wt and *Epac1*^{-/-} mice, ^{aa}*P* = .0035, ^{bbb}*P* = .0007, ^c*P* = .031, ^d*P* = .018, ^e*P* = .037, ^f*P* = .039, ^{gg}*P* = .0051, ^h*P* = .044).

feeding led, as expected,²⁷ to increased diuresis in both Wt and *Epac1*^{-/-} mice, but it did not enhance the *Epac1*^{-/-} diuretic phenotype (Table 2B). Further, switching from 4% to 40% protein had opposite effects in *Epac1*-deleted and *UT-A1/3*-deleted mice²⁷ regarding water consumption, urine production and urine osmolarity (Figure S2). The level of *UT-A1/3* (*Slc14a2*) mRNA was similar in Wt and *Epac1*^{-/-} mice both 3 hours after WL and 6 hours after WL and dDAVP injection (Figure S3A).

The increased diuresis of the *Epac1*^{-/-} mice at low or moderate protein load was matched by increased water intake (Tables 1 and 2A) resulting in similar retention of water for either strain. To rule out any effect of compulsory drinking behaviour, mice were denied access to drinking water. Dehydration was counteracted by intragastric infusion of 1.5-mL water (WL) at the onset of each experiment. We found a significantly higher 6-hour urine output for *Epac1*^{-/-} than for

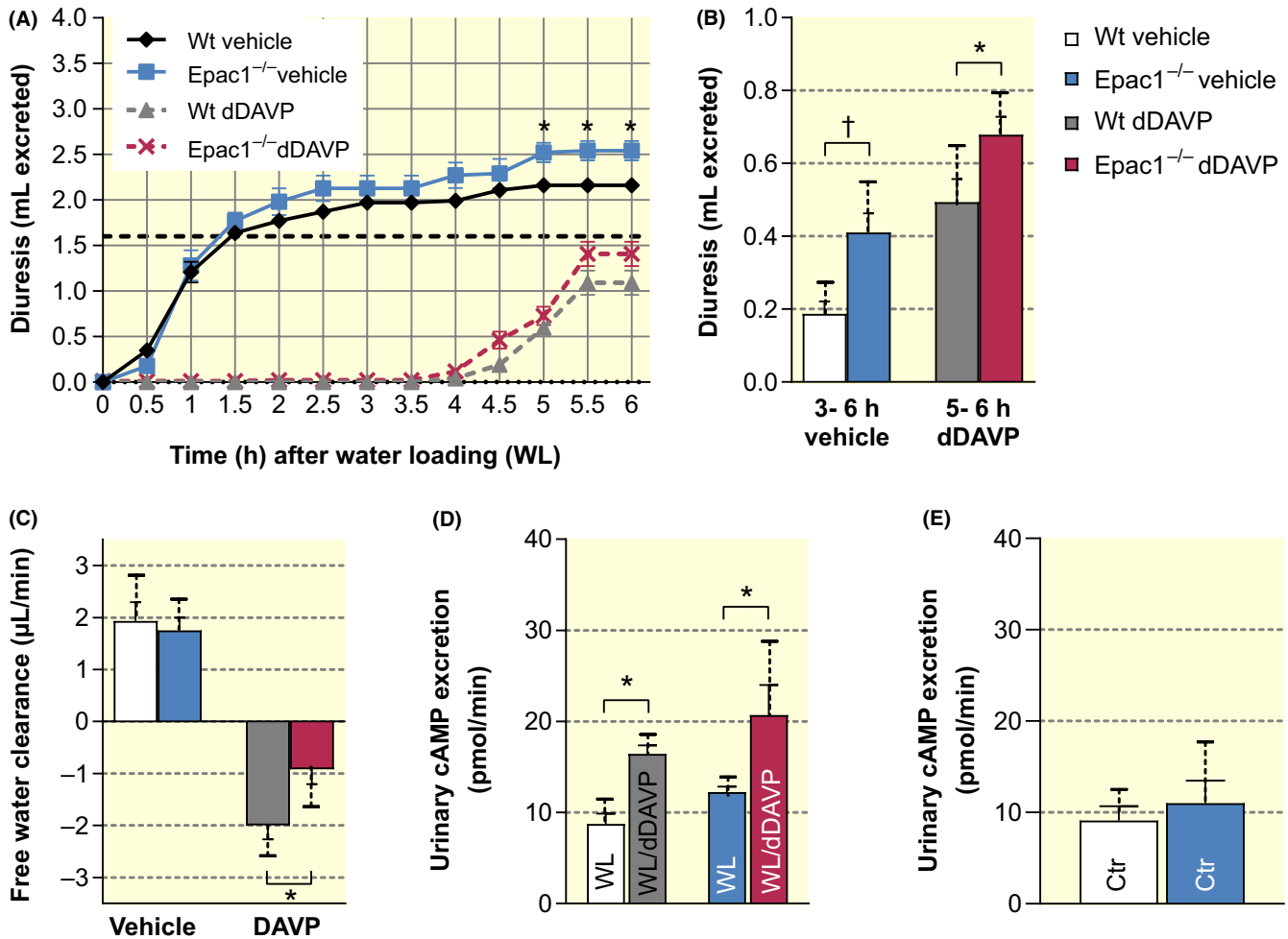


FIGURE 1 Epac1^{-/-} mice have higher diuresis and spare less free water than Wt mice under antidiuretic conditions. (A) Accumulative diuresis during the first 6 h after water loading (WL) alone or after injection of dDAVP. The horizontal hatched line represents the volume (1.5-mL H₂O + 0.1-mL saline) loaded, $n = 6-7$ mice/group, $^*P = .016$ at 5h, $^*P = .015$ at 5.5 h and $^*P = .015$ at 6 h. (B) The diuresis between 3 and 6 h after WL alone and between 5 and 6 h for WL + dDAVP, $n = 5-6$ mice/group, $^{\dagger}P = .0058$ for vehicle and $^*P = .045$ for dDAVP. (C) Free water clearance ($\mu\text{L min}^{-1}$), $n = 6$ mice/group, $P = .69$ for vehicle and $^*P = .023$ for dDAVP. (D) cAMP excretion (pmol min^{-1}), $n = 5-7$ mice/group, $F(1, 20) = 0.043$, $P = .84$ for interaction and $^{\ddagger}P = .0003$ for treatment (E) cAMP excretion (pmol min^{-1}) for control mice, $n = 5-7$ mice/group, $P = .58$. Values are presented as mean \pm SEM (panel A) or as both mean (SD) and mean (SEM) (panels B-E). Unpaired two-tailed Student's *t* test with Welch's correction when applicable (A-C, E) or two-way ANOVA with Tukey's adjustment for multiple comparisons (D) was used to determine statistical differences between Wt and Epac1^{-/-} mice in the various treatment groups. For further details, see Figure 9 and Materials and Methods

Wt mice (Table S2, 4% protein feeding), especially between 3 and 6 hours after WL (Figure 1A,B).

2.2 | Epac1^{-/-} mice have impaired urinary concentrating capacity under antidiuretic conditions, but intact dDAVP-induced increase of cAMP and AQP-2

The water-loaded Wt and Epac1^{-/-} mice had similar diuresis until the WL had been eliminated (Figure 1A). Only thereafter did the Epac1^{-/-} mice have higher urine excretion than Wt mice (Figure 1A,B). To test whether Epac1^{-/-} mice were

subresponsive to AVP, they were given a bolus injection of dDAVP. Although both Wt and Epac1^{-/-} mice had a period of complete anuria after dDAVP + WL, the diuresis recovered slightly earlier for Epac1^{-/-} than for Wt mice (Figure 1A,B). Analysis of the urine revealed that the Epac1 null mice had higher free water clearance than Wt mice (Figure 1C).

The subresponsiveness of the Epac1 null mice to AVP/dDAVP could be due to deficient Avpr2-mediated increase of cAMP or of AQP-2. Both cAMP excretion (Figure 1D,E) and expression of Aqp2 mRNA or AQP-2 protein (Figure S3B-D) were similar in Wt and Epac1^{-/-} mice, under basal conditions as well as after dDAVP stimulation.

2.3 | Epac1^{-/-} mice have lower papilla and bladder urine osmolarity than Wt mice under antidiuretic conditions

The Epac1^{-/-} mouse water-sparing deficiency could be explained by a perturbed renal corticopapillary osmotic gradient. The length of the renal papillary tip as well as the thickness of the papillary base, medulla and cortex appeared similar in Epac1^{-/-} and Wt mice upon dissection. Moreover, the papillary blocks, dissected in the same way from Wt and Epac1^{-/-} mice, had similar average dry weight (Figure 2A).

The water content increased significantly from cortex to papilla for either Epac1^{-/-} mice (74.3%-83.8%, [‡]*P* < .001) or Wt mice (73.8%-80.8%, [†]*P* = .004), but slightly more so (by about 9.5%) for Epac1 null mice than (about 7%) for Wt mice (Figure 2B). More strikingly, the papillary Na⁺ content of Epac1^{-/-} was only 53% of that in Wt (Figure 2C).

To evaluate whether the difference was related to less endogenous AVP stimulation in the Epac1^{-/-} mice, the plasma Na⁺ concentration and osmolarity were determined. We found similar values for Epac1^{-/-} (152(SD6) mmol/L Na; 324(SD7) mosm Kg⁻¹) and Wt mice (152(SD3) mmol/L Na; 328(SD8) mosm Kg⁻¹).

To establish the correlation between papillary and urine content of osmolytes, we analysed also the urine aspirated from the bladder of overnight water-deprived mice just before the kidney sampling. The urine from Epac1^{-/-} mice had only 59% (SD18) as high urea concentration and 58% (SD14) as high osmolarity as Wt mouse urine (Figure 3). The reduction of the urine concentration of the various osmolytes was similar to the reduction of Na⁺ in the papilla (Figures 2 and 3).

2.4 | Epac1^{-/-} and WT mice have similar extravasation of albumin

In a previous study, Epac1^{-/-} mice had increased leakage from microvessels in skin, intestine and skeletal muscle as measured using the double isotope ¹²⁵I-HSA and ¹³¹I-HSA injection method (see Ref. 7 for details). We found no difference in albumin permeability between Wt and Epac1^{-/-} mice. The Epac1^{-/-} mice also failed to increase permeability in response to ANP, which increases albumin permeability in Wt mouse skin, muscle and intestine⁷ (Figure 4A,B).

2.5 | The CD TJs are shorter and less dense in Epac1^{-/-} than in Wt mice

The corticopapillary osmotic gradient perturbation of Epac1 null mice (Figures 2 and 3) resembled that reported in mice with genetically induced CD TJ 'leakiness' associated with less E-cadherin expression.²⁶ The striking CD clustering of mRNA coding for Avpr2, Epac1 and the downstream Epac1 target E-cadherin⁶ (Table S3) prompted a study of the CD junctions. To know if the Epac1 null mice had altered CD JCs, we compared Epac1^{-/-} mouse CD junctions with Wt controls using TEM.

Epac1^{-/-} and Wt CD had similar general paracellular organization (see Figure 5 for representative examples), with an apical TJ that merges into a JC. Morphometric analysis of 56 PC/PC junctions from six Wt mice and 51 PC/PC junctions from five Epac1^{-/-} mice revealed that compared to Wt the Epac1^{-/-} TJs were on average shorter, less dense (had higher electron transmittance) and associated with less electron-dense junctional material (Table S4, Figure 6A-C). A similar, but less strong, trend was found for the JC (Table S4). Table S4 lists also the percentage of each TJ appearing to be 'open', as subjectively,

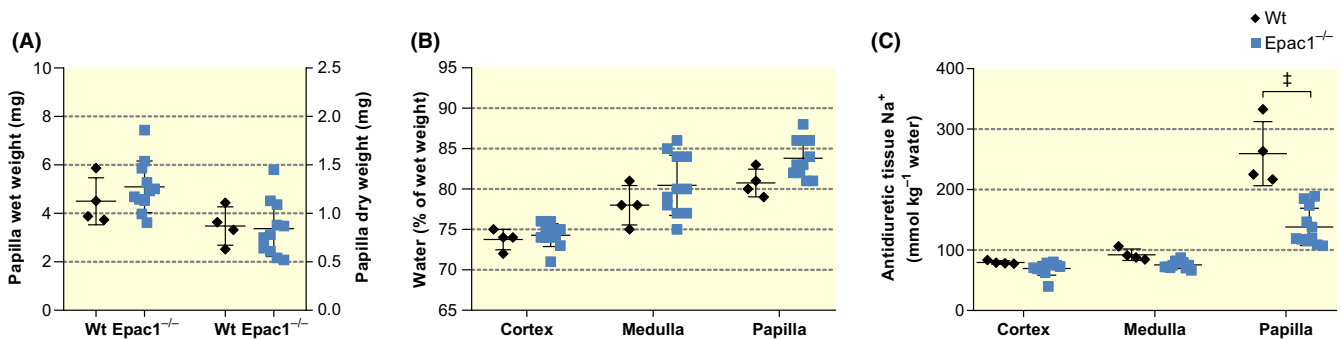


FIGURE 2 Content of water and Na⁺ in cortex, medulla and papilla. (A) The wet and dry weight of similarly sampled tissue blocs from papilla of Wt or Epac1^{-/-} mice. (B) The water content (%) in consecutively sampled tissue blocks from cortex, medulla and papilla. (C) The sodium concentration in consecutively sampled tissue blocs from cortex to papilla in Wt and Epac1^{-/-} mice. The values shown are mean (SD), n = 4 Wt mice and n = 11 Epac1^{-/-} mice. Unpaired two-tailed Student's *t* test (A) wet weight, *P* = .35 and dry weight, *P* = .86 or two-way ANOVA with Sidak's adjustment for multiple comparisons (B) *F*(1, 39) = 5.717, ^{*}*P* = .0217 and (C) *F*(1, 39) = 42.1, [‡]*P* < .001 was used to determine statistical differences between Wt and Epac1^{-/-} mice

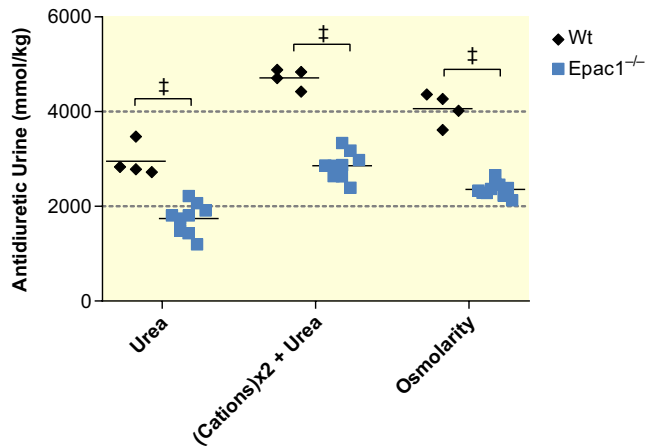


FIGURE 3 The osmolarity of antidiuretic urine from Wt and $Epac1^{-/-}$ mice. The figure shows at left the concentration of urea and at right the (actual) osmolarity of urine from overnight water-restricted Wt (black symbols) or $Epac1^{-/-}$ (blue symbols) mice. In the middle, the urea concentration + 2× the sum of the determined cation concentrations (sodium + ammonium + potassium + calcium + magnesium) is shown. The values are mean, $n = 4$ for Wt mice and $n = 11$ for $Epac1^{-/-}$ mice. Two-way ANOVA with Sidak's adjustment for multiple comparisons, $F(1, 34) = 287.2$, $^{\ddagger}P < .001$, was used to determine statistical differences between Wt and $Epac1^{-/-}$ mice

and blindly scored by independent operators (Table S4; see also Figure 5). The median value for this parameter was 0 for Wt and 38% for $Epac1$ null mouse TJs (Table S4).

The ICs have been reported to have very high²⁸ or quite low²⁹ $Epac1$ expression. We found that intercalated/principal (IC/PC) TJs were longer and more electron dense than PC/PC TJs, and less affected by $Epac1$ deletion (Figure S4A-C,

Table S5) than those in the PC/PC paracellular space (Table S4).

2.6 | $Epac1^{-/-}$ mice have intact glomerular filtration barrier and moderately elevated GFR

Rodent glomeruli have high $Epac1$ mRNA expression,⁶ suggesting that $Epac1$ has a functional role in the glomerulus. We probed this possibility, first by testing whether $Epac1^{-/-}$ mice could have a defect glomerular filtration barrier, a dysfunction of which would cause increased albumin leakage.^{30,31} We found similar levels of albumin in Wt and $Epac1^{-/-}$ mice urine, and whether the mice had been treated with dDAVP or not (Figure 7).

We considered next if $Epac1$ could control the GFR, possibly by modulating the TGF loop at the glomerular end. This possibility was tested by comparing the renal clearance of creatinine and of [¹⁴C]inulin in the absence and presence of the TGF-blocking agent furosemide. To know if the primary furosemide target (NKCC2 of the *macula densa*) was intact in $Epac1^{-/-}$ mice, we compared first the effect of furosemide on Wt and $Epac1$ null mouse diuresis and Na^+ excretion.

We found that Wt and $Epac1^{-/-}$ mice had similar furosemide-induced diuresis and Na^+ excretion (Figure 8A,B). The furosemide-treated Wt and $Epac1^{-/-}$ mice had also similar clearance of creatinine and inulin (Figure 8C,D). In the absence of furosemide, the $Epac1^{-/-}$ mice had increased clearance of creatinine, inulin and cAMP under both basal and dDAVP-stimulated conditions (Figure 8C,D; Table 3, Figure S5A,B).

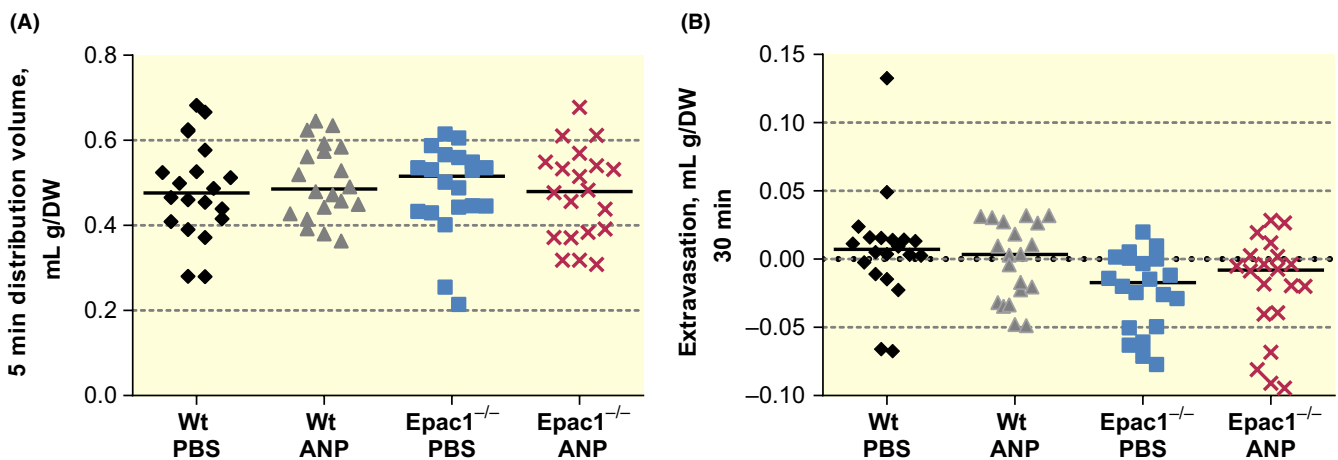


FIGURE 4 The renal content of ¹³¹I-albumin (iv injected at -5 min) and ¹²⁵I-albumin (iv injected at -35 min). (A) The content of ¹³¹I-HSA per mg dry weight of kidney removed 5 min after the intravenous injection of ¹³¹I-HSA. Each group comprised 10 animals, for each of which both the right and left kidney were analysed. A horizontal line indicates the median value. (B) The difference between the renal ¹²⁵I-HSA and ¹³¹I-HSA content of mice injected 35 min earlier with ¹²⁵I-HSA and 5 min earlier with ¹³¹I-HSA. The values shown are mean (SD). One-way ANOVA with Dunnett's adjustment for multiple comparisons, (A) $P = .94$ and (B) $P = .16$, was used to determine statistical differences between Wt and $Epac1^{-/-}$ mice

3 | DISCUSSION

Our observation that *Epac1* null mice have nephrogenic *diabetes insipidus* (Table 1A, Figure 1) with lowered papillary Na^+ content (Figure 2C) and shorter and less dense CD TJs (Table S3, Figures 5 and 6) conforms to the hypothesis that the primary *Epac1*-dependent antidiuretic mechanism is to control the leakiness of the intercellular junction between CD PCs. Possible *Epac1*-dependent mechanisms modulating transcellular water and urea transport or glomerular filtration appear to be less significant to explain the *diabetes insipidus* phenotype. These observations provide new understanding of the biological significance of high renal *Epac1* expression.⁶⁻⁸ We discuss the possible

Epac1-dependent mechanisms suggested in the introduction in more detail below.

The diuretic phenotype with decreased conservation of free water (Figure 1C) is a hallmark of deficient AVP action in the CD.^{23,32} We tested several mechanisms that could lead to decreased AVP-mediated water conservation. We found no evidence that *Epac1*^{-/-} mice have a subresponsive *Avpr2* receptor or excessive degradation of cAMP. The renal cAMP excretion after a general dDAVP stimulation increased at least as much in *Epac1*^{-/-} as in Wt mice (Figure 1D). The secretory component (clearance—GFR) for cAMP was similar in Wt and *Epac1*^{-/-} mice (Figure S5B), implying that Wt and *Epac1*^{-/-} mice have similar renal excretion of cAMP. The apparent cAMP resistance of *Epac1*^{-/-} mice to AVP effects

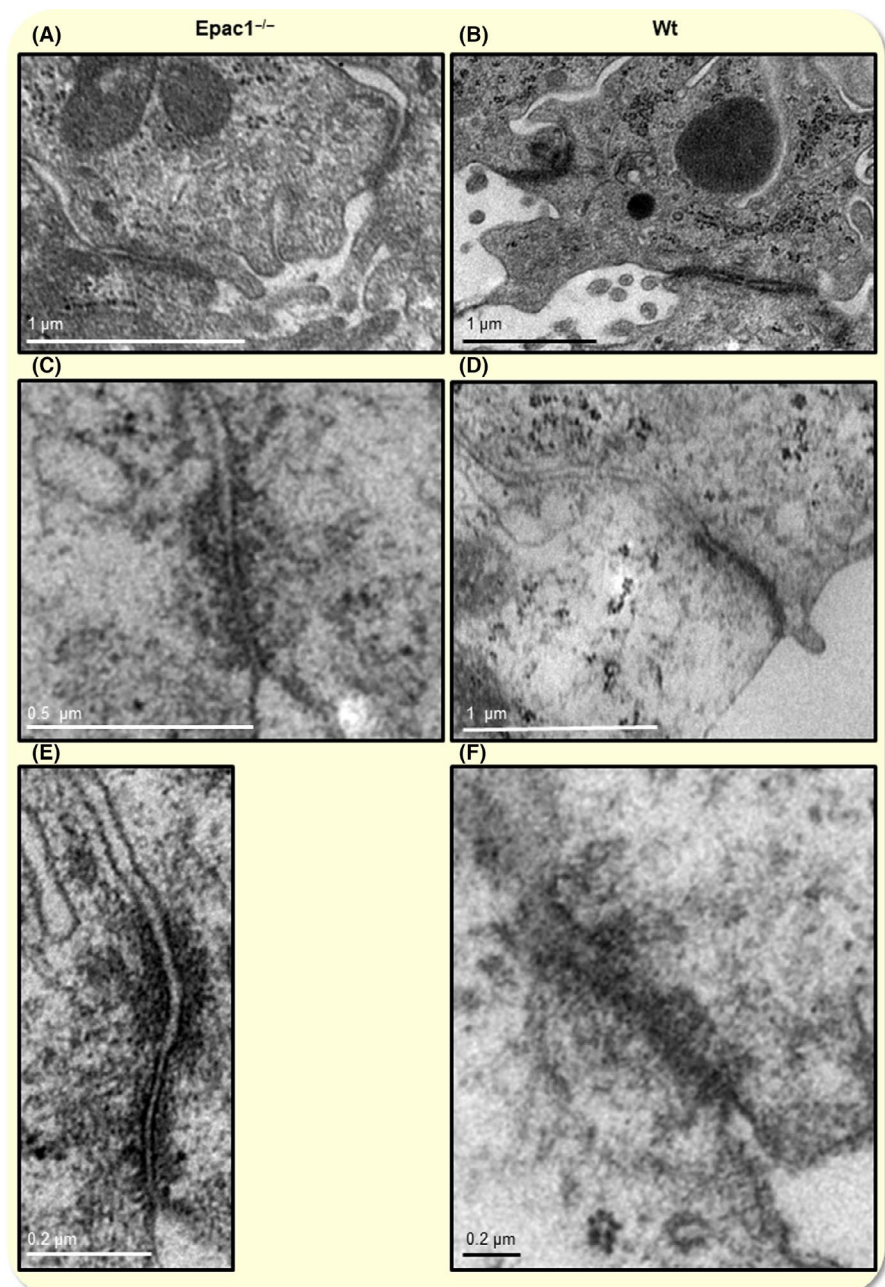


FIGURE 5 The ultrastructure of typical CD tight junctions from *Epac1*^{-/-} and Wt mice. (A, C, E) Junctions from three *Epac1*^{-/-} mice with near median TJ length and electron density. The morphometric data for each of the sections are found in Table S4, where they are highlighted in blue and marked with *. (B, D, F) Junctions from three representative Wt mice, highlighted in yellow and marked with * in Table S4. CD, collecting duct

was, therefore, not explained by increased cellular cAMP extrusion.

The CD and connecting tubule (CNT) segments of the nephron have the highest expression of both Epac1 (*RapGef3*) and AVP receptor 2 (*Avpr2*), while the short (SDL) and long (LDLIM) descending limb and tAL segments of the nephron have moderate Epac1 (*RapGef3*) expression and no appreciable *Avpr2* expression (Ref. 6 Table S3). Thus, Epac1 is likely to be activated by AVP mainly in the CD and CNT segments.

The action of Epac1 in the cAMP-stimulated CD could be to augment the known PKA-mediated actions such as induction or membrane insertion of aquaporins 2, 3 or UT-A1/3 or UT-A2.^{5,13} Although Epac1 has been reported to promote AQP-2 expression upon long-term cAMP stimulation,¹⁴ neither the Aqp-2 transcript nor the protein level differed between Wt and Epac1 null mice (Figure S3B-D). Thus, direct Epac1-dependent regulation of AQP-2 expression is unlikely to account for the diuretic state.

The diuretic Epac1^{-/-} phenotype was not explained by deficient urea transport, since it was more severe at low (4%) than high (40%) protein diet (Table 2), and not associated with altered expression of the UT-A1/3 urea transporter (Figure S3A). A lack of Epac1 does, therefore, not lead to diet/urea-induced osmotic diuresis in contrast to the expectation from an in vitro study¹³ reporting Epac1 enhanced UT-A1/3 urea transporter expression.

Overnight water-deprived Epac1^{-/-} mice had not only a more dilute bladder urine than Wt mice (Figure 3), but also a similarly decreased renal medullary Na⁺ and presumably osmotic gradient (Figure 2C). Epac1 therefore appears to

be required to maintain a steep medullary osmotic gradient to prevent water loss under antidiuretic conditions. A similar osmotic gradient deficiency was observed in mice with lowered CD paracellular TJ resistance due to CD-specific deletion of the transcription factor GRHL2.²⁶ The similar decrease of Na⁺ and osmolarity in the renal papilla and urine in GRHL2- and Epac1-targeted mice (²⁶ and Figures 2 and 3), as compared to Wt mice, argues that water can

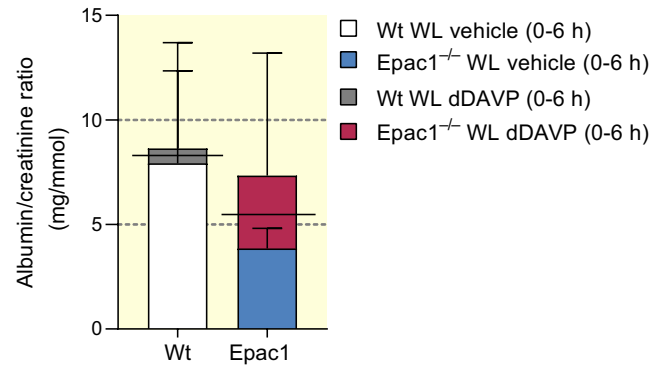


FIGURE 7 Urinary albumin excretion. Albuminuria, expressed as the urine albumin/creatinine ratio, is shown for Wt ($n = 4$) and Epac1^{-/-} ($n = 4$) mice given vehicle or dDAVP. The urine was collected for 6 h after WL (see Figure 1 for details of method). The values shown are mean (SD). Solid thin lines show the average for vehicle- and dDAVP-injected mice. Unpaired two-tailed Student's t test with Welch's correction and unpaired two-tailed Student's t test, $P = .16$ for WL vehicle and $P = .75$ for WL dDAVP was used to determine statistical differences between Wt and Epac1^{-/-} mice. WL, water loading

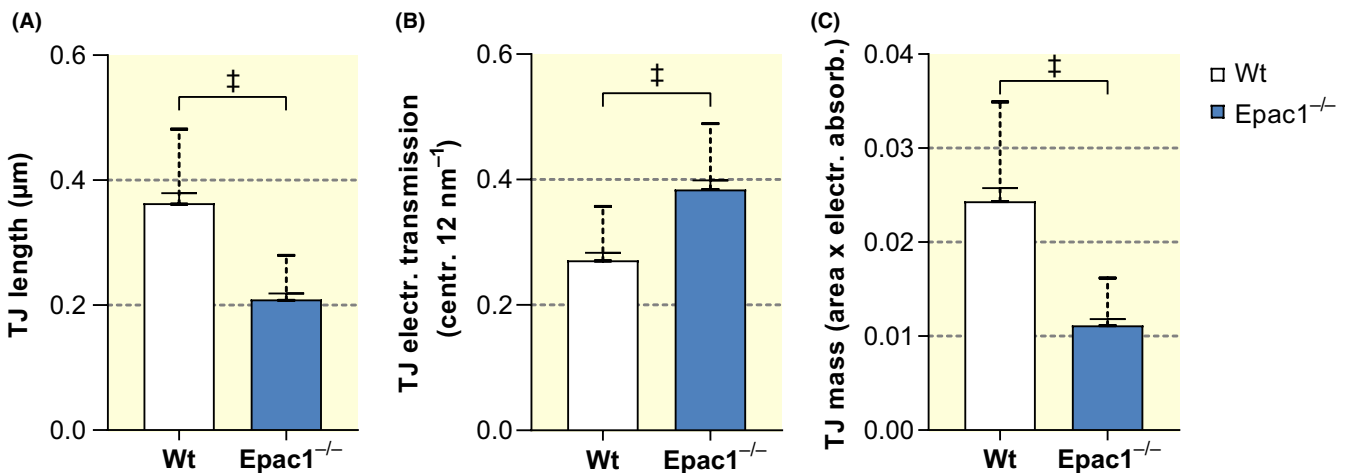


FIGURE 6 The CD tight junctions are shorter and less dense in Epac1^{-/-} than in Wt mice. (A) Histograms of the TJ length of Wt and Epac1^{-/-} collecting duct PC/PC junctions. (B) Histogram of the average central electron transmission, determined along the entire length of each tight junction. (C) Histogram of the average TJ 'mass'. The central electron transmission (B) is the average value observed along the central region of the TJ divided by the transmission in the collecting duct lumen. The TJ 'mass' is the TJ area \times the average TJ electron absorbance (see Materials and Methods section for details). Values are shown as mean (SD) and mean (SEM), $n = 6$ Wt mice and 5 Epac1^{-/-} mice. A total of 56 Wt TJs and 51 Epac1^{-/-} mouse junctions were analysed. Details of statistics used: Two-tailed Mann-Whitney test (A) Sum of ranks 4112, 1666, Mann-Whitney $U = 340$, $^{\ddagger}P < .001$, (B) sum of ranks 1762, 4016, Mann-Whitney $U = 166$, $^{\ddagger}P < .001$ and (C) sum of ranks 4126, 1652, Mann-Whitney $U = 326$, $^{\ddagger}P < .001$. CD, collecting duct; PC, principal cell

equilibrate between the papillary tissue and the pre-urine in the CD lumen. Such equilibration would not be expected if Epac1 were critically required for aquaporin synthesis or insertion. In line with the observation above, there was no difference between Epac1^{-/-} and Wt mice regarding AQP-2 expression (Figure S3).

Isolated GRHL2-deficient PC cells have severely decreased paracellular electrical resistance.²⁶ This observation provides a link between paracellular ‘leakage’ and the in vivo phenotype of decreased papillary osmotic gradient and increased diuresis,²⁶ but it does not tell if the PC TJ permeability can be under physiological control.

We found that the PC/PC TJs were less electron-dense and had less associated junctional material in Epac1^{-/-} than Wt mice (Figures 5 and 6; Table S4). Epac1 is well known to tighten JCs, both in vitro (see Ref. 25 for recent review) and in vivo.⁷ It may also mediate the cAMP-induced stabilization of the retinal blood brain barrier TJs.³³ The simplest explanation of the present Epac1 null mouse

diuretic phenotype is, therefore, that Epac1 maintains the corticopapillary osmotic gradient by strengthening the CD paracellular TJs.

The diuretic Epac1^{-/-} phenotype described here, and preliminarily reported,⁹ is characterized by dilute urine under antidiuretic conditions, as well as near unaltered Na⁺ excretion (Table 2). Therefore, it differs strongly from the recently described Epac1^{-/-} osmotic diuresis phenotype, caused by increased Na⁺ excretion ascribed to decreased proximal tubule (PT) expression of the sodium-hydrogen exchanger 3.^{34,35} Although a PT-localized primary phenotype is plausible in view of an early study showing strong immunohistochemical staining for Epac1 in the PT brush border,²⁸ it is not supported by more recent quantitative mRNA expression data, which show insignificant *RapGef3* expression in the PT (Table S3,⁶). There is no obvious explanation for the dramatic difference of renal phenotypes between the two *RapGef3* ‘knock out’ mice. The mice used in the present study have increased

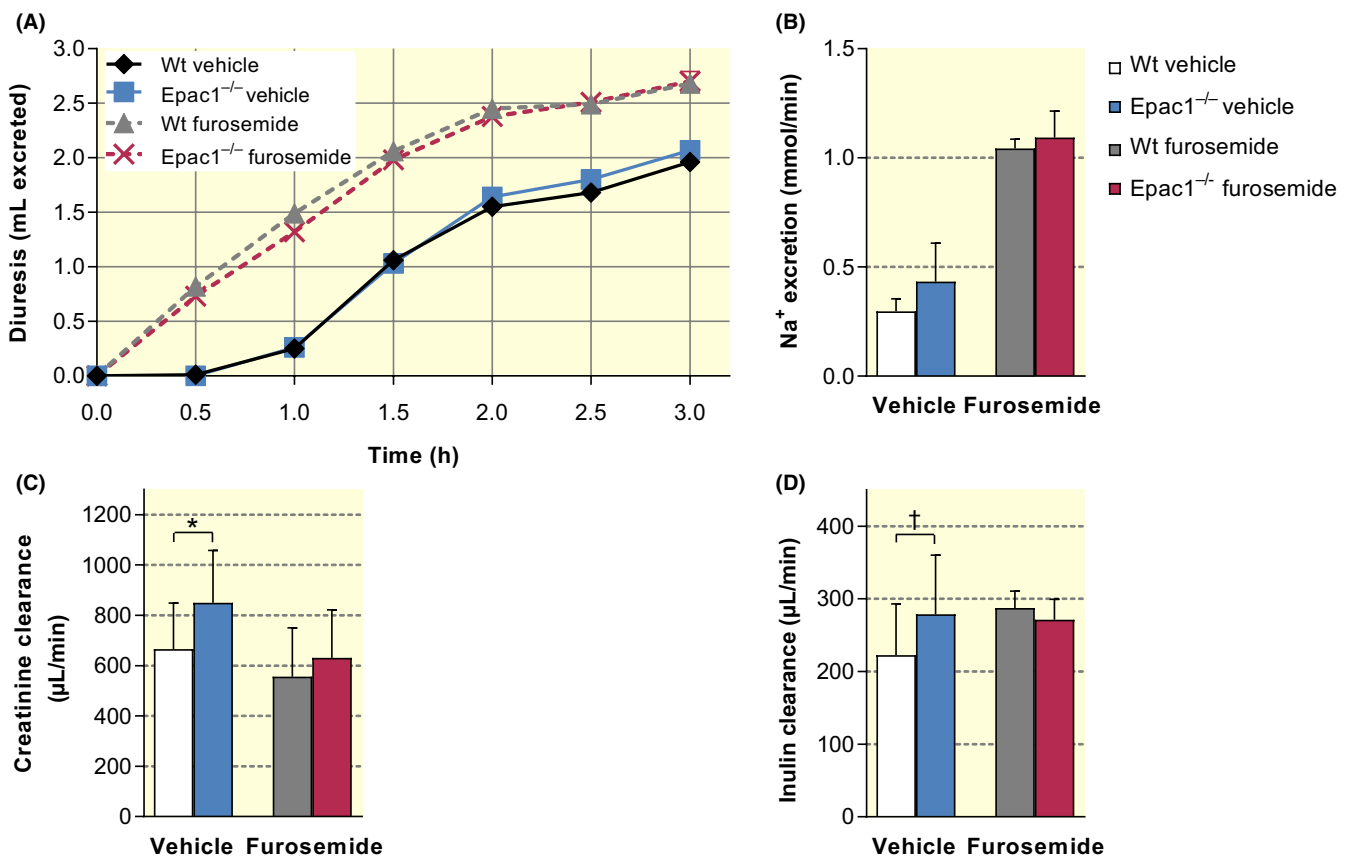


FIGURE 8 The effect of furosemide on diuresis, Na⁺, creatinine and inulin clearance. (A, B, C) Wt (n = 11) and Epac1^{-/-} (n = 11) mice were water loaded (see Figure 1A for details), and the urine collected continuously for 3 h. Four days later, the water loading (WL) was repeated, combined with furosemide injection. The effect of furosemide is shown for (A) diuresis, (B) Na⁺ excretion rate, n = 3–4 mice/group, P = .19 for vehicle and P = .47 for furosemide. (C) The creatinine clearance of Wt (n = 10–14) and Epac1^{-/-} mice (n = 10–13) during the first 6 h after WL, with or without a concomitant furosemide injection, *P = .022 for vehicle and P = .40 for furosemide. (D) The effect of furosemide on inulin clearance (for four pairs of vehicle or furosemide treated Wt and Epac1^{-/-} mice), †P = .0017 for vehicle and P = .22 for furosemide. Values are mean ± SEM (A) or mean (SD). Unpaired two-tailed Student’s *t* test was used for statistics, except for panel (C) where the paired two-tailed Student’s *t* test was used. For further details, see Materials and Methods

microvascular permeability, as would be expected based on extensive *in vitro* studies on endothelial cells with downregulated Epac1 activity (see review Ref. 25). Further, endothelial cells isolated from the Epac1^{-/-} mice used here have increased junctional permeability when monolayers are tested *in vitro*³⁶ implying that the permeability phenotype is caused by the lack of Epac1 in the endothelial cells and not by an altered *in vivo* environment in the Epac1^{-/-} mice.

The high *RapGef3* mRNA expression in rat glomeruli⁶ suggests that Epac1 can impact glomerular functions. Epac1 appeared not to be required to maintain an intact glomerular filtration barrier since the Epac null mice did not have albuminuria (Figure 7).

The Epac1 null mice had increased clearance of creatinine and cAMP (Table 3, Figure 8C and Figure S5), which could be explained either by increased tubular excretion^{37,38} or increased GFR. The lower [¹⁴C]inulin clearance of Wt than Epac1^{-/-} mice, in the absence, but not in the presence, of the TGF inhibitor furosemide (Figure 8D) suggests that Epac1 may restrain the GFR via TGF modulation.

In conclusion, Epac1 appears to prevent *diabetes insipidus* mainly by maintaining the corticomedullary osmotic

gradient. This may at least in part be achieved through Epac1-mediated control of paracellular CD ‘leakage’.

4 | MATERIALS AND METHODS

4.1 | Reagents

Creatinine, dDAVP and furosemide were obtained from Sigma-Aldrich. ¹⁴C-inulin (1 mCi) was from Perkin-Elmer (Cetus) and was diluted with unlabelled inulin (from chicory, Sigma-Aldrich) before being used for experiments in a concentration of 2.1 mCi mL⁻¹. Ultracel-30 membrane filters (cut-off = 30.000 kDa) were from Millipore.

4.2 | Ethical approval

The animal experiments were approved by the Norwegian Animal Research Authority and conducted according to the European Convention for the Protection of Vertebrates Used for Scientific Purposes, Norway. These regulations comply with the UK policies and regulations.³⁹ The Animal Care

TABLE 3 Key urinary and plasma parameters for Wt and Epac1^{-/-} mice on normal chow given 1.5-mL water load (WL) ± dDAVP

Variable determined	WL + vehicle, day 1		dDAVP injection day 7	
	WT	Epac1 ^{-/-}	WT	Epac1 ^{-/-}
Urine output (mL 6h ⁻¹)	2.16 (SD0.16)	2.59 (SD0.29) ^{aa}	1.02 (SD0.32)	1.41 (SD0.33)
Diuresis—loaded H ₂ O (μL g ⁻¹)	29.5 (SD4.9)	46.4 (SD12) ^b	-22.8 (SD16)	-3.41 (SD14)
Urine osm. (mOsm kg ⁻¹ H ₂ O)	223 (SD40)	256 (SD21)	599 (SD143)	441 (SD92)
Urine urea (mmol/L)	126 (SD24)	124 (SD23)	275 (SD76)	211 (SD56)
Urine Na ⁺ (mmol/L)	39.1 (SD6.7)	45.1 (SD3.4)	76.4 (SD35)	48.4 (SD15)
Urine K ⁺ (mmol/L)	19.9 (SD3.9)	23.0 (SD4.6)	51.5 (SD20)	35.6 (SD12)
Urine creatinine (μmol/L)	331 (SD74)	332 (SD44)	961 (SD271)	864 (SD328)
Urine cAMP (μmol/L)	3.15 (SD1.03)	4.44 (SD0.54) ^c	5.91 (SD0.83)	8.35 (SD2.36) [§]
nosm (excr. min ⁻¹ g ⁻¹)	60.3 (SD7.7)	78.2 (SD4.7) ^{ddd}	75.4 (SD6.1)	70.0 (SD7.7)
nmol Urea (excr. min ⁻¹ g ⁻¹)	34.0 (SD5.4)	37.7 (SD6.1)	34.8 (SD5.3)	34.1 (SD8.4)
nmol Na ⁺ (excr. min ⁻¹ g ⁻¹)	2.65 (SD0.38)	3.49 (SD0.67)	9.60 (SD4.2)	8.06 (SD2.3)
nmol K ⁺ (excr. min ⁻¹ g ⁻¹)	1.34 (SD0.21)	1.75 (SD0.32)	6.39 (SD1.5)	5.56 (SD0.97)
pmol creatinine (excr. min ⁻¹ g ⁻¹)	92.4 (SD15)	101 (SD5.7)	125 (SD22)	140 (SD45)
Plasma urea (mmol/L)	11.2 (SD0.0)	10.5 (SD0.0)	10.8 (SD1.8)	10.2 (SD2.4)
Plasma creatinine (μmol/L)	7.9 (SD0.4)	6.7 (SD0.7) ^{ee}	5.70 (SD1.1)	5.72 (SD1.5)
Plasma cAMP (nmol/L)	60.9 (SD4.4)	63.1 (SD1.7)	69.9 (SD5.0)	59.7 (SD8.0)
Urea clearance (μL min ⁻¹)	67.6 (SD15)	84.9 (SD17)	66.8 (SD18.0)	84.8 (SD21.1)
Creatinine clearance(μL min ⁻¹)	243 (SD69)	353 (SD34) ^{ff}	472 (SD18)	557 (SD159)

Wt (n = 6) and Epac1^{-/-} mice (n = 6) were water loaded (1.5 mL) and injected with 0.1-mL saline. Thereafter, the urine collected for 6 h, when blood was sampled for plasma analysis. One week later, the same mice injected with dDAVP instead of saline. Data are mean (SD) and excretion data are normalized per g body weight. The statistical significance was judged by unpaired Student's *t* test with Welch' correction when applicable, either for vehicle-treated (^{aa}*P* = .0096, ^b*P* = .0114, ^c*P* = .022, ^{ddd}*P* = .0007, ^{ee}*P* = .0037, ^{ff}*P* = .0056) or dDAVP-treated animals ([§]*P* = .038).

and Use Programs at University of Bergen are accredited by AAALAC international.

4.3 | Targeted disruption of the *Epac1* gene to produce C57BL/6J *Epac1*^{-/-} mice

The C57BL/6JBomTac mouse strain is described at <http://www.taconic.com/wmspage.cfm?parm1=764>. *Epac1* null (*Epac1*^{-/-}) mice were generated using the Cre-LoxP system as described previously.^{7,40,41} In short, *loxP* sites were inserted by homologous recombination into the gene encoding *Epac1* (*RapGef3*) flanking exons 7-10. These exons encode the CBD-B domain, which codes for the only functional cAMP site of *Epac1*.^{42,43} In addition, a frame shift was introduced distal to the deletion in order to minimize the probability of expression of truncated *Epac1* fragments through unscheduled translation. C57BL/6JBomTac mice

from Taconic, Denmark were used to backcross the recombinant chimeric mice for at least 10 generations. The stability of the deletion was confirmed by genotyping for each new generation.

4.4 | General animal handling

The mice used in the present study were about 3-4 months old females, weighing 18-30 g. The wild-type C57BL/6J BomTac mice (Wt) and their *Epac1* null counterparts (*Epac1*^{-/-}) were littermates, or they were born and kept in neighbour cages of the *Epac1*^{-/-} mice. They were generally housed 4-5 mice together in IVC-II cages (Sealsafe® IVC Blue Line 1284L, Tecniplast) and maintained under standard housing conditions at 21°C ± 0.5°C, 55% ± 5% humidity, 12-hours artificial light-dark cycle (150 lux). The *Epac1* null mice had the same weight as their Wt littermates, from which they were indistinguishable

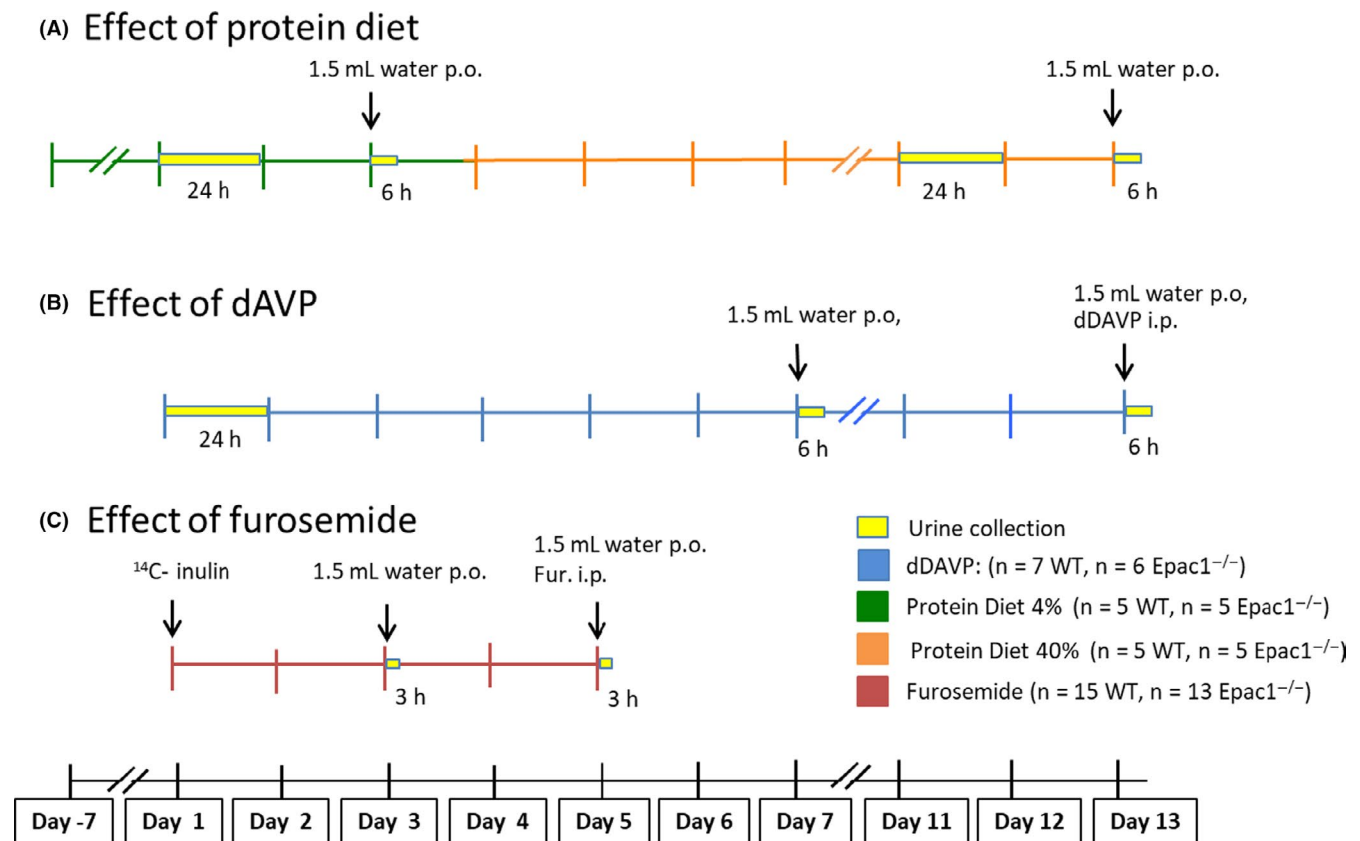


FIGURE 9 Overview of the experiments conducted to test the effect on urine production and composition of protein diet, dDAVP and furosemide. A, Mice were fed low (4%) protein diet for 7 d and the urine sampled for 24 h thereafter. One day later, the mice received an acute per-oral (p. o.) intubation of 1.5-mL water, and the urine was collected continuously (as voided) for 6 h thereafter. The animals were next switched to high-protein (40%) diet, and 7 d thereafter, subjected to the same experiments as when fed low-protein diet. B, Mice fed standard (12.5%) protein diet were transferred to metabolic cages and their urine collected for 24 h under basal conditions. Seven days later, the mice received a 1.5-mL water load (WL) and 0.1-mL saline i.p., and their urine was collected continuously for 6 h thereafter. The experiment was repeated after 7 d, but with injection of dDAVP instead of saline. C, Mice, inserted sc. on the back 3 d previously with a mini-osmotic pump loaded with [¹⁴C]inulin, were water loaded as described above, and the urine collected for 3h. Two days later, the experiment was repeated, but with a furosemide injection at the time of water loading

based on visual observation under standard housing conditions. The Wt and Epac1 null mice had also similar blood pressure.⁷

For most experiments, the mice were provided with standard rodent chow containing 12.5% protein (Special Diet Services RM1, 801151, Scanbur BK) and water ad libitum. For experiments designed to manipulate the standard urea load, the animals received low (4%) protein or high (40%) protein chow from Custom Diet Services, Special Diet Services, Witham, UK. Since most experiments were conducted in single-housed metabolic cages, each animal was acclimatized for 24 hours in a metabolic cage for 3-4 days before the onset of each experiment.

Anaesthesia was with 1.5%-2% Isoba[®] vet. Isoflurane (Schering-Plough Animal Health) under continuous flow of O₂ (1 L m⁻¹) and N₂O (1 L m⁻¹). The anaesthetized animals were placed on a heating pad at 37°C to limit any drop of the body temperature. The dDAVP (1-ng g⁻¹ body weight) or furosemide (40-µg g⁻¹ body weight) was injected intraperitoneal (i.p.) in 0.1-mL 150-mmol/L aqueous saline (NaCl) solution during anaesthesia shortly before the intragastric intubation with 1.5-mL water (see Figure 9 below for details). Cardiac blood (0.4 mL) was aspirated into a 0.5-mL syringe with 0.1-mL citrate-dextrose solution by cardiac puncture of animals killed with CO₂, and thereafter centrifuged for 3 minutes at 500 rpm to yield plasma. Plasma samples were stored at -80°C and urine samples at -20°C for further analysis.

The animals showed no symptoms of distress or illness during the experiments. Two Epac1^{-/-} mice appeared debilitated during a 24-hours pre-experimental stay in metabolic cages. They were therefore excluded from any experiment. Two mice (one Wt and one KO) had badly fitted drinking bottles during the 24-hours experiment, resulting in contamination of urine. They were excluded from that experiment, but not from the subsequent water-loading experiments.

4.5 | Overview of the major animal experiments conducted

4.5.1 | Urine collection and WL

In one series of experiments, the urine of animals given chow with various protein content was collected for 24 hours via a tube connected to the funnel-shaped bottom of the metabolic cage. The experiments were conducted in individual MMC10 metabolic cages (Hatteras Instruments, Inc) and started at 09.00 AM. The urine bladders were emptied by bladder massage immediately before placing the animals in the metabolic cages.

In another series, each mouse was anaesthetized just after the bladder had been emptied, and then subjected to acute water loading (WL, 1.5-mL H₂O) by intragastric

intubation through a 38-mm metal gavage with a silicon tip (AgnTho's AB), and placed in a metabolic cage. The urinary bladder was emptied by external massage before the urine was collected (see Materials and Methods and legend to Figure 9 for further details). In this way, errors caused by individual differences of recent water intake and residual urine content were minimized. The urine that was spontaneously voided thereafter was collected into a siliconized beaker and manually recovered by pipetting. The volume of each recovered urine sample was determined, before adding it to a pre-weighed tube. The sum of the volumes determined fit well with the weight increase of the collecting tube.

4.5.2 | Experiments using high protein diet-induced urea loading

To test the ability of the mice to handle urea loading, they were first fed low protein diet for 1 week in ordinary cages, and thereafter for 24 hours in individual metabolic cages. The mice were next water loaded as described above, returned to the metabolic cage and the urine voided was collected during a period of 6 hours. Thereafter, 0.2-mL whole blood was collected from a puncture in the facial vein for analysis of serum creatinine and urea. The next week, the same mice were switched to high protein diet, and thereafter treated as described for the low protein fed mice.

4.5.3 | Determination of GFR and microvascular permeability

The GFR was determined as the renal clearance of [¹⁴C]inulin as described in,⁴⁴ except that the infusion pumps (Alzet[®] osmotic minipump model 1007D, DURECT Corporation) were placed subcutaneously between the withers rather than intraperitoneally. Each pump was filled with 25 µCi [¹⁴C]inulin in 150-mmol/L aqueous saline (NaCl) solution, and delivered 0.5 ± 0.1 µL h⁻¹. They were primed overnight in the 0.9% saline solution at 37°C. Experiments were conducted at least 2 days after pump implantation. The amount of [¹⁴C]inulin was determined in the urine and in whole blood collected from the facial vein in 10-µL capillary pipettes (Minicaps, Hirschmann-Laborgeräte). For terminal experiments, the blood (2 × 50 µL) was collected by heart puncture. Samples of urine (10 µL), plasma (28 µL) or whole blood (50 µL) were mixed thoroughly with 1-mL 2% SDS (20 g SDS L⁻¹) and next with 10-mL scintillation liquid (Emulsifier-safe[™], Perkin-Elmer, Inc) before being counted in Tri-Carb 2900TR Liquid Scintillation Analyzer (Perkin-Elmer, Inc). To minimize any non-specific chemiluminescence, the vials were left for 1 day in

the dark before starting the counting, and each vial was counted 3×10 minutes. The counting efficiency of [^{14}C] inulin was determined by recounting each vial after a small volume with a known high [^{14}C]inulin concentration had been added to each vial.

A previous study comparing Wt and *Epac1*^{-/-} mice⁷ showed that *Epac1* and ANP acted oppositely on the microvascular permeability for albumin in tissues like skin, fat, muscle and intestine, with known capacity to store excess intravascular fluid. Similar data for the kidney were obtained, but not reported. They are reported here since they could tell whether *Epac1* deletion or ANP affects the extravascular renal accumulation of serum albumin. The mice were anaesthetized with 1.5%-2% isoflurane in air (Isoba vet, Schering-Plough Animal Health) administered through a nose cone. Human serum albumin (HSA) labelled with either ^{125}I or ^{131}I was injected sequentially in the jugular vein, respectively, 35 and 5 minutes prior to termination of the experiment. Blood samples were obtained before the mice received a lethal iv injection of saturated KCl, and tissue samples harvested. The right and left kidneys were removed, rinsed for blood, the radioactivity determined and spillover from ^{131}I to ^{125}I corrected for. The kidneys were dried until stable dry weight was obtained. Distribution volumes were determined as plasma equivalent volumes (ie cpm per g tissue divided by cpm per mL plasma obtained at the end of the experiment for each mouse) and referenced to dry tissue weight. For further details, see Ref. 7.

4.6 | Determination of the osmolarity and the concentration of NaCl and selected other ions in the renal papilla interstitium and in bladder urine

Eleven female *Epac1*^{-/-} mice and four Wt mice, deprived of drinking water overnight (total 10 hours), were anaesthetized with 1.5% isoflurane (IsoFlo[®]Vet 100%, ABBOT Laboratories Ltd) in 100% O₂. Bladder urine was collected by suprapubic puncture and collected in Eppendorf tubes for measuring osmolarity (Wescor vapor pressure osmometer model 5600) and the concentration of urea (mixed-mode chromatography) and cations (ion chromatography). Blood was collected by heart puncture and both kidneys were then rapidly removed through a midline incision and snap-frozen in Eppendorf tubes in liquid nitrogen. The kidney poles of the shock-frozen kidneys were cut-off perpendicularly to the long axis with a scalpel. The remaining central 2- to 3-mm thick tissue block containing the papilla was then immediately dissected on a chilled glass plate into a pyramidal-shaped tissue block with the papillary tip as the apex and the cortex as the basis. From this block, three consecutive tissue samples were cut-off while still semi-frozen separating the

pale papilla from the darker medulla and cortex from the remaining medulla.

The tissue samples were immediately transferred into pre-weighed Eppendorf tubes, weighed and dried at 40°C for estimation of water content. The dried tissue samples were then equilibrated in 500- μL Milli-Q water in the same Eppendorf tubes for at least 3 days to measure total tissue cation content. Sodium, ammonium, potassium, magnesium and calcium in diluted urine (1:201), plasma (1:101) and undiluted eluate from renal papilla, medulla and cortex were baseline separated in a 10 minutes 7.5-60 mmol/L MSA gradient by a Dionex IonPac CS 12A analytical column (8.5 μm , 2×250 mm, P/N 046075) at a flow rate of 0.2 mL min⁻¹ using a Dionex Integriion HPIC System equipped with a CDRS 600 (2 mm) Cation Electrolytic Suppressor and a high pressure EGC 500 methane sulfonic acid eluent generator cartridge. Urea in urine was separated in an acetonitrile-water gradient using a Thermo Scientific[™] Acclaim[™] Trinity P2 column (100 mm, catalogue number 085434) connected to a Thermo Scientific UltiMate 3000 Rapid Separation system and detected by a Corona Veo Charged Aerosol Detector.

4.7 | Laboratory methods

Urinary and plasma cAMP was determined as described previously.^{45,46} The urea concentration in urine was determined by the QuantiChrom[™] Kit (DIUR-500; Bio-Assay systems) according to manufacturer's protocol. To achieve accurate determination of urea in mouse plasma, the samples were diluted fivefold in H₂O and partially deproteinized by spinning through Ultracel-30kDa membrane filters (Millipore), before being assayed. Osmolality was determined using a Wescor 133 vapor pressure osmometer with SS-033 filter discs (Wescor Inc) according to the manufacturer's protocol. Urine Na⁺ and K⁺ were determined using ion-selective electrodes (analysed by the Laboratory for Clinical Biochemistry at Haukeland Hospital in Bergen, Norway).

Creatinine in urine was determined either by an enzymatic creatinase assay (CREA Plus kit; Boehringer Mannheim), using a Roche Cobas Bio Analyzer (Roche) or based on HPLC.²⁰ Only the latter method, with the modifications described below, produced reliable determinations in mouse plasma. Briefly, plasma samples (20 μL) were deproteinized by adding 2-mL acetonitrile, vortexed and centrifuged for 15 minutes at 13 000 *g* at 4°C. After evaporation to dryness, the samples were dissolved in 120 μL of 5-mmol/L sodium acetate, pH 5 (HPLC mobile phase), and 15 μL of 20 000 \times g supernatant injected into a 100 \times 1.45-mm PRP-X200 cation exchange column (Hamilton) equilibrated with HPLC mobile phase to separate creatinine, which is positively charged at

pH 4.68, from acidic interfering compounds. By switching to 10-mmol/L potassium buffer (pH 7.10) in the second-dimension column (Proswift SCX-1S, 4.6 × 50 mm, Dionex), the creatinine molecule was neutralized, resulting in a reduced retention and a sharp, well-defined peak detected at its absorption maximum of 234. The specificity of the method was validated by the analysis of urine and plasma samples before and after treatment at 25°C overnight with 90 U mL⁻¹ creatinase (EC 3.5.2.10, 1000 U) and 50 U mL⁻¹ creatinase (EC 3.5.3.3, 500U).

Albumin from 10- μ l urine was determined by 2D-HPLC using size-exclusion chromatography (Super SW2000, 4.6 × 300 mm, Tosoh Bioscience) in the first dimension and reversed phase chromatography (Proswift Rp4H 1 × 50 mm, Dionex) in the second dimension. The albumin from the first-dimension column was automatically loaded onto the second-dimension column at a flow rate of 0.35 mL min⁻¹ by an inline switch. Albumin was then separated from proteins with similar molecular weight by an 8-minute acetonitrile gradient (5-60%). The albumin concentration was determined based on the area under the curve for standards and samples.⁴⁷

The relative Aqp-2 and UT-A1/3 mRNA levels were determined by quantitative qRT-PCR. Total RNA was isolated from whole kidneys from WL (+3 hours) and WL/dDAVP (+6 hours) Wt and Epac1^{-/-} mice using the TRIzol reagent according to the manufacturer's protocol. 1.5 μ g RNA was converted to cDNA using 0.75 μ mol/L random hexamer and 1.5 μ mol/L Oligo-dT primer, 1-mmol/L dNTP-mix and 50 U RevertAid Reverse Transcriptase (Thermo Scientific). The RT-PCR reaction was carried out on MJ Research PTC-200 for four cycles at 25°C for 10 minues, 42°C for 60 minues, 70°C for 10 minues and 4°C 'forever'. The qPCR was on a LightCycler 480 II (Roche) with cDNA corresponding to 5.5 ng RNA and SYBR Green Supermix (BioRad) with one 300 seconds cycle at 95°C, 40 cycles of 10 seconds at 95°C, 10 seconds at 60°C and 20 seconds at 72°C followed by a melting curve analysis. All results are average of two separate experiments, each in triplicate. Expression levels were related to the sample (total) RNA concentration as well as to the geometrical mean concentration of the assumedly stably expressed ('household') mRNA's coding for succinate dehydrogenase complex subunit alpha (SDHA), Peptidyl-prolyl cis-trans isomerase A (Ppia) and cGMP-dependent protein kinase (Pkg1), and relative gene expression estimated using the 1.8^{- $\Delta\Delta$ Ct} method. The primer sequences for: AQP-2; fwd: GCCCTGCTCTCTCCATTG, rev: TCAAACCTGCCAGTGACAAC, for UT-A1; fwd: CTGCCA CCTGGGCTTCTTTTG, rev: GGGTAACGCCTGAGAGA CAAG, for SDHA; fwd: CATGCCAGGGAAGATTACAA, rev: GCACAGTCAGCCTCATTCAA, for Ppia; fwd: TGAGCACT GGAGAGAAAGGA, rev: CCATTATGGCGTGTAAGTCA and for Pkg1; fwd: TGGATGACGTTTCCAACAAA, rev: CACTATGTGGCGCTTCTTGA.

Immunoblotting of AQP-2: For this, 100 μ g of whole kidney extracts in RIPA buffer containing cOMplete™ Mini Protease Inhibitor Cocktail (Roche Diagnostics GmbH) was separated by 4%-12.5% (w/vol) SDS/PAGE and transferred to Hybond™ P 0.45 μ m PVDF membrane (GE Healthcare Life Sciences, Buckinghamshire, UK) using rabbit anti-AQP-2 (1:3000 in PBS-T o/n) as primary antibody and alkaline phosphatase-conjugated goat anti-rabbit IgG (1:10 000 in PBS-T, 1 hour RT, A3687, Sigma-Aldrich) as the secondary antibody. Prof. Robert A. Fenton, University of Aarhus, Denmark kindly provided the primary antibody. The membranes were incubated in 100-mmol/L aqueous diethanolamine with 100-mmol/L MgCl₂ pH 9.5 for 2 × 2 minues before the blots were developed with ECL using CDP-Star® Chemiluminescent Substrate (Tropix) and evaluated with the Luminescent Image Analyzer LAS-3000 (Fujifilm). Relative intensity of the bands was quantified and normalized to a loading control (β -actin) using the software Multi Gauge volume 2.3.

Haematoxylin and eosin (H&E) staining: Formalin-fixed, paraffin-embedded kidney sections (4 μ m) were stained with H&E as described in.⁴⁸ Kidney histology was visualized by light microscopy (Leica, DMLB) and analysis Pro. 3.2 software (Leica). Images 10x-20x was taken using a Leica DC300 camera.

The TEM study was performed essentially as described earlier.⁷ Briefly, kidney medulla tissue was pre-fixed in 2% glutaraldehyde in 0.1 mol/L Na-cacodylate buffer o/n at 4°C, washed 3 × 30 minues in 0.1 mol/L Na-cacodylate buffer and post-fixed for 2 hours in 1% OSO₄ in 0.1 mol/L Na-cacodylate buffer at 4°C. The samples were then washed for 3 × 30 minues in 0.1 mol/L Na-cacodylate buffer, dehydrated in a graded alcohol series and embedded in a graded 1.2 Propylene oxide/Agar 100 Resin series, ending with pure Agar 100 Resin o/n at RT. After 48 hours curing at 60°C, ultrathin sections (55-60 nm) were stained with uranyl acetate and lead citrate. The mounted samples were studied in a JEOL JEM-1230 TEM (JEOL Ltd), at the Molecular Imaging Center at UoB.

4.8 | Morphometric analysis of CD paracellular junctions

The electron micrographs of the renal medulla CD paracellular apical TJ and its adjoining JC were analysed for length, area and density using the ImageJ software (vers. 2.0; <https://imagej.net>) The average pixel density was determined for the central 12-18 nm of the (apical) TJ and the central 18-24 nm of the adjoining JC. We determined also the average pixel density for the whole area of each TJ and JC, including their attached electron-dense material, which was clearly demarcated from the ordinary cytoplasm and therefore easy to delineate. Since the overall exposure varied between the micrographs, the junctional pixel density (a) was adjusted for the pixel density in the CD lumen

(b). The parameter 'el.transm' in Table S4 is therefore a/b (TJ pix. dens./CD lumen 'background' pix. dens). The subjective estimation of TJ 'openness' was assessed by two independent persons. All sections were evaluated blindly.

4.9 | Graphic illustration and statistical analysis

Excel 2014/2017 (Microsoft Corporation) and GraphPad Prism 6.0 (Graph-Pad Software) were used for statistical calculations and graphic illustrations. Data sets are generally presented as mean (SD) and mean (SEM). For comparison of variables in littermate animals relative to the *Epac1*^{-/-} animals, statistical significance was assessed by either of the following tests: the unpaired two-tailed Student's *t* test with Welch's correction (when applicable), the paired two-tailed Student's *t* test, the one-way ANOVA with Dunnett's adjustment for multiple comparisons, two-way ANOVA with Sidak's or Tukey's adjustment for multiple comparisons, the Kruskal-Wallis test with Dunn's multiple comparisons test, the two-tailed Mann-Whitney test or Wilcoxon matched-pairs signed rank sum test. We confirm that the material submitted agree with the Good Publishing Practice in Physiology.⁴⁹

ACKNOWLEDGEMENTS

We are grateful to Nina L. Larsen and Endy Spriet for their expert technical help.

CONFLICT OF INTEREST

The authors declare no conflict of interest.

AUTHOR CONTRIBUTIONS

RB, RK, BH, MB, SD, OT, KSÅ, LP: Planning and execution of experiments; SD, RB, OT, KSÅ, RR, CR, TK, FC: Preparation of manuscript. All authors read and approved the final manuscript.

DATA AVAILABILITY STATEMENT

The data that support the findings of this study are available from the corresponding author upon reasonable request.

ORCID

Kathrine Sivertsen Åsrud  <https://orcid.org/0000-0001-7951-4044>

Rolf K. Reed  <https://orcid.org/0000-0002-2633-6595>

Olav Tenstad  <https://orcid.org/0000-0001-5833-2620>

Stein O. Døskeland  <https://orcid.org/0000-0002-4009-4756>

<https://orcid.org/0000-0002-4009-4756>

REFERENCES

- Bos JL. Epac proteins: multi-purpose cAMP targets. *Trends Biochem Sci.* 2006;31(12):680-686.
- Kopperud R, Krakstad C, Selheim F, Døskeland SO. cAMP effector mechanisms. Novel twists for an 'old' signaling system. *FEBS Lett.* 2003;546(1):121-126.
- Kleppe RML, Herfindal L, Selheim F, Døskeland SO. Assessing cyclic nucleotide recognition in cells: opportunities and pitfalls for selective receptor activation. Chapter 4. In: Cheng X ed. *Cyclic Nucleotide Signaling*. CRC Series on Methods in Signal Transduction. Boca Raton, FL, London, New York, NY: Press, Taylor & Francis; 2015:61-80. ISBN 1482235560.
- Taylor SS, Buechler JA, Yonemoto W. cAMP-dependent protein kinase: framework for a diverse family of regulatory enzymes. *Annu. Rev. Biochem.* 1990;59:971-1005.
- Robichaux WG 3rd, Cheng X. Intracellular cAMP Sensor EPAC: physiology, pathophysiology, and therapeutics development. *Physiol Rev.* 2018;98(2):919-1053.
- Lee JW, Chou CL, Knepper MA. Deep sequencing in microdissected renal tubules identifies nephron segment-specific transcripts. *J Am Soc Nephrol.* 2015;26(11):2669-2677.
- Kopperud RK, Rygh CB, Karlsen TV, et al. Increased microvascular permeability in mice lacking Epac1 (*Rapgef3*). *Acta Physiol (Oxf).* 2017;219(2):441-452.
- de Rooij J, Zwartkruis FJ, Verheijen MH, et al. Epac is a Rap1 guanine-nucleotide-exchange factor directly activated by cyclic AMP. *Nature.* 1998;396(6710):474-477.
- Bjørnstad R. *Characterization of the Renal Function in Epac1 (RapGef3) Knockout Mice* [Master]. Bergen, Norway: University of Bergen Library: Department of Biomedicine; 2014.
- Christensen AE, Selheim F, de Rooij J, et al. cAMP analog mapping of Epac1 and cAMP kinase. Discriminating analogs demonstrate that Epac and cAMP kinase act synergistically to promote PC-12 cell neurite extension. *J Biol Chem.* 2003;278(37):35394-35402.
- Schwede F, Bertinetti D, Langerijs CN, et al. Structure-guided design of selective Epac1 and Epac2 agonists. *PLoS Biol.* 2015;13(1):e1002038.
- Frohlich O, Klein JD, Smith PM, Sands JM, Gunn RB. Regulation of UT-A1-mediated transepithelial urea flux in MDCK cells. *Am J Physiol Cell Physiol.* 2006;291(4):C600-606.
- Wang Y, Klein JD, Blount MA, et al. Epac regulates UT-A1 to increase urea transport in inner medullary collecting ducts. *J Am Soc Nephrol.* 2009;20(9):2018-2024.
- Kortenoeven ML, Trimpert C, van den Brand M, Li Y, Wetzels JF, Deen PM. In mpkCCD cells, long-term regulation of aquaporin-2 by vasopressin occurs independent of protein kinase A and CREB but may involve Epac. *Am J Physiol Renal Physiol.* 2012;302(11):F1395-1401.
- Yip KP. Epac-mediated Ca(2+) mobilization and exocytosis in inner medullary collecting duct. *Am J Physiol Renal Physiol.* 2006;291(4):F882-890.
- Herfindal L, Nygaard G, Kopperud R, Krakstad C, Døskeland SO, Selheim F. Off-target effect of the Epac agonist 8-pCPT-2'-O-Me-cAMP on P2Y12 receptors in blood platelets. *Biochem Biophys Res Comm.* 2013;437(4):603-608.
- Poppe H, Rybalkin SD, Rehmann H, et al. Cyclic nucleotide analogs as probes of signaling pathways. *Nat Methods.* 2008;5(4):277-278.
- Fenton RA, Knepper MA. Mouse models and the urinary concentrating mechanism in the new millennium. *Physiol Rev.* 2007;87(4):1083-1112.
- Schnermann J, Briggs JP. Tubuloglomerular feedback: mechanistic insights from gene-manipulated mice. *Kidney Int.* 2008;74(4):418-426.

20. Haslene-Hox H, Oveland E, Berg KC, et al. A new method for isolation of interstitial fluid from human solid tumors applied to proteomic analysis of ovarian carcinoma tissue. *PLoS ONE*. 2011;6(4):e19217.
21. Tucker BJ, Blantz RC. Effect of furosemide administration on glomerular and tubular dynamics in the rat. *Kidney Int*. 1984;26(2):112-121.
22. Curry FE, Taxt T, Rygh CB, et al. Epac1^(-/-) mice have elevated baseline permeability and do not respond to histamine as measured with dynamic contrast-enhanced magnetic resonance imaging with contrast agents of different molecular weights. *Acta Physiol (Oxf)*. 2019;225(3):e13199.
23. Moses AM. Osmotic thresholds for AVP release with the use of plasma and urine AVP and free water clearance. *Am J Physiol*. 1989;256(4 Pt 2):R892-897.
24. Pannekoek WJ, Kooistra MR, Zwartkruis FJ, Bos JL. Cell-cell junction formation: the role of Rap1 and Rap1 guanine nucleotide exchange factors. *Biochim Biophys Acta*. 2009;1788(4):790-796.
25. Radeva MY, Waschke J. Mind the gap: mechanisms regulating the endothelial barrier. *Acta Physiol (Oxf)*. 2018;222:e12860.
26. Hinze C, Ruffert J, Walentin K, et al. GRHL2 is required for collecting duct epithelial barrier function and renal osmoregulation. *J Am Soc Nephrol*. 2018;29(3):857-868.
27. Fenton RA, Flynn A, Shodeinde A, Smith CP, Schnermann J, Knepper MA. Renal phenotype of UT-A urea transporter knockout mice. *J Am Soc Nephrol*. 2005;16(6):1583-1592.
28. Li Y, Konings IB, Zhao J, Price LS, de Heer E, Deen PM. Renal expression of exchange protein directly activated by cAMP (Epac) 1 and 2. *Am J Physiol Renal Physiol*. 2008;295(2):F525-533.
29. Chen L, Lee JW, Chou CL, et al. Transcriptomes of major renal collecting duct cell types in mouse identified by single-cell RNA-seq. *Proc Natl Acad Sci USA*. 2017;114(46):E9989-E9998.
30. Haraldsson B, Nystrom J, Deen WM. Properties of the glomerular barrier and mechanisms of proteinuria. *Physiol Rev*. 2008;88(2):451-487.
31. Scott RP, Quaggin SE. Review series: the cell biology of renal filtration. *J Cell Biol*. 2015;209(2):199-210.
32. Hirano T, Yamamura Y, Nakamura S, Onogawa T, Mori T. Effects of the V(2)-receptor antagonist OPC-41061 and the loop diuretic furosemide alone and in combination in rats. *J Pharmacol Exp Ther*. 2000;292(1):288-294.
33. Ramos CJ, Lin C, Liu X, Antonetti DA. The EPAC-Rap1 pathway prevents and reverses cytokine-induced retinal vascular permeability. *J Biol Chem*. 2018;293(2):717-730.
34. Cherezova A, Tomilin V, Buncha V, et al. Urinary concentrating defect in mice lacking Epac1 or Epac2. *FASEB J*. 2019;33(2):2156-2170.
35. Tomilin VN, Pochynyuk O. A peek into Epac physiology in the kidney. *Am J Physiol Renal Physiol*. 2019;317(5):F1094-F1097.
36. Mariya Yosifova Radeva KS, Ponce AG, Døskeland S-O, Curry FE, Reed RK, Waschke J. Epac1 is required for cAMP-mediated endothelial barrier stabilization. Abstract presented at Experimental Biology 2019 Meeting; 1.April 2019; 2019.
37. Eisner C, Faulhaber-Walter R, Wang Y, et al. Major contribution of tubular secretion to creatinine clearance in mice. *Kidney Int*. 2010;77(6):519-526.
38. Vallon V, Eraly SA, Rao SR, et al. A role for the organic anion transporter OAT3 in renal creatinine secretion in mice. *Am J Physiol Renal Physiol*. 2012;302(10):F1293-F1299.
39. Drummond GB. Reporting ethical matters in the Journal of Physiology: standards and advice. *J Physiol*. 2009;587(Pt 4):713-719.
40. Nygaard G, Herfindal L, Asrud KS, et al. Epac1-deficient mice have bleeding phenotype and thrombocytes with decreased GPIIb/IIIa expression. *Sci Rep*. 2017;7(1):8725.
41. Aesoy R, Muwonge H, Asrud KS, et al. Deletion of exchange proteins directly activated by cAMP (Epac) causes defects in hippocampal signaling in female mice. *PLoS ONE*. 2018;13(7):e0200935.
42. Rehmann H, Rueppel A, Bos JL, Wittinghofer A. Communication between the regulatory and the catalytic region of the cAMP-responsive guanine nucleotide exchange factor Epac. *J Biol Chem*. 2003;278(26):23508-23514.
43. Rehmann H. Characterization of the activation of the Rap-specific exchange factor Epac by cyclic nucleotides. *Methods Enzymol*. 2006;407:159-173.
44. Jobin J, Bonjour JP. Measurement of glomerular filtration rate in conscious unrestrained rats with inulin infused by implanted osmotic pumps. *Am J Physiol*. 1985;248(5 Pt 2):F734-F738.
45. Doskeland SO, OGREID D. Ammonium sulfate precipitation assay for the study of cyclic nucleotide binding to proteins. *Methods Enzymol*. 1988;159:147-150.
46. Jensen BO, Kleppe R, Kopperud R, et al. Dipyridamole synergizes with nitric oxide to prolong inhibition of thrombin-induced platelet shape change. *Platelets*. 2011;22(1):8-19.
47. Semaeva E, Tenstad O, Skavland J, et al. Access to the spleen microenvironment through lymph shows local cytokine production, increased cell flux, and altered signaling of immune cells during lipopolysaccharide-induced acute inflammation. *J Immunol*. 2010;184(8):4547-4556.
48. Cardiff RD, Miller CH, Munn RJ. Manual hematoxylin and eosin staining of mouse tissue sections. *Cold Spring Harbor Protoc*. 2014;2014(6):655-658.
49. Persson PB. Good publication practice in physiology 2015. *Acta Physiol*. 2015;215(4):163-164.

SUPPORTING INFORMATION

Additional supporting information may be found online in the Supporting Information section.

How to cite this article: Sivertsen Åsrud K, Bjørnstad R, Kopperud R, et al. Epac1 null mice have nephrogenic diabetes insipidus with deficient corticopapillary osmotic gradient and weaker collecting duct tight junctions. *Acta Physiol*. 2020;229:e13442. <https://doi.org/10.1111/apha.13442>